



HAL
open science

Asymmetry during a horizontal annular flow in a micro-channel: optical measurements and effect of dimensionless numbers

C. Capo, T. Layssac, S. Lips, A. W. Mauro, R. Revellin

► **To cite this version:**

C. Capo, T. Layssac, S. Lips, A. W. Mauro, R. Revellin. Asymmetry during a horizontal annular flow in a micro-channel: optical measurements and effect of dimensionless numbers. *Journal of Physics: Conference Series*, 2017, 796 (1), pp.012045. 10.1088/1742-6596/796/1/012045 . hal-01487694

HAL Id: hal-01487694

<https://hal.science/hal-01487694v1>

Submitted on 20 Mar 2019

HAL is a multi-disciplinary open access archive for the deposit and dissemination of scientific research documents, whether they are published or not. The documents may come from teaching and research institutions in France or abroad, or from public or private research centers.

L'archive ouverte pluridisciplinaire **HAL**, est destinée au dépôt et à la diffusion de documents scientifiques de niveau recherche, publiés ou non, émanant des établissements d'enseignement et de recherche français ou étrangers, des laboratoires publics ou privés.

Asymmetry during a horizontal annular flow in a micro-channel: optical measurements and effect of dimensionless numbers

This content has been downloaded from IOPscience. Please scroll down to see the full text.

2017 J. Phys.: Conf. Ser. 796 012045

(<http://iopscience.iop.org/1742-6596/796/1/012045>)

View [the table of contents for this issue](#), or go to the [journal homepage](#) for more

Download details:

IP Address: 134.214.140.132

This content was downloaded on 13/03/2017 at 06:56

Please note that [terms and conditions apply](#).

You may also be interested in:

[Systematic Enhancements of Switching Rate in Intrinsic Josephson Junctions](#)

Y Nomura, T Mizuno, H Kambara et al.

[Liquid flow in a micro-channel](#)

S-S Hsieh, C-Y Lin, C-F Huang et al.

[Numerical Simulation of the Roll Forming Process of Aluminum Folded Micro-channel Tube](#)

Tianxia Zou, Ning Zhou, Yinghong Peng et al.

[A position-sensitive micro-channel plate detector with a parallel-strip resistive anode and integrated charge-sensitive amplifiers](#)

W. Wang, D. Yu, J. Liu et al.

[Flow boiling of a new low-GWP refrigerant inside a single square cross section microchannel](#)

S Bortolin and D Del Col

[Neon helium mixtures as a refrigerant for the FCC beam screen cooling: comparison of cycle design options](#)

S Kloeppel, H Quack, C Haberstroh et al.

[A new type of diabatic flow pattern map for boiling heat transfer in microchannels](#)

R Revellin and J R Thome

[Compressor Lubrication -the key to Performance](#)

Sonny G Sundaresan

Asymmetry during a horizontal annular flow in a micro-channel: optical measurements and effect of dimensionless numbers

C CAPO¹, T LAYSSAC², S LIPS², A W MAURO^{1,3} and R REVELLIN²

¹ Federico II University of Naples, Department of Industrial Engineering, P. le Tecchio, 80, 80125, Naples (Italy)

² CETHIL UMR5008, Université de Lyon, CNRS, INSA-Lyon, F-69621, Villeurbanne (France)

³ e-mail: alfonsowilliam.mauro@unina.it

Abstract. New applications of HFC refrigerants in organic Rankine cycles at high saturation temperatures and the wider use of CO₂ for air-conditioning have pushed research to the characterization of two-phase heat transfer at medium/high reduced pressures and have pointed out the effect of these operating conditions on asymmetric distribution of refrigerant around tube perimeter and its indirect effect on heat transfer. Currently there is a lack of data about asymmetric distribution of liquid film at the wall, especially for refrigerants and micro-channels. In order to have a physical evidence of this asymmetry also for micro-channels and approach to a relationship between this phenomenon and dimensionless parameters, new data are here presented. The asymmetric annular flow of the refrigerant R245fa inside a horizontal, round 2.95 mm inner diameter channel is studied with pictures captured by a high speed video camera. The experimental results here presented were obtained at saturation temperatures equal to 20 °C and 40 °C at low mass velocities (50, 100 and 200 kg m⁻²s⁻¹) to asymmetric distribution, enriching the database presented in previous studies. The new dimensionless parameter, eccentricity, has been related to the dimensionless groups: Froude and Bond numbers, and Martinelli parameter, showing the mutual correlation among them.

1. Introduction

Two-phase flows are encountered in many industrial applications related to heat transfer process or to fluid transport such as evaporators and condensers for the refrigeration and air-conditioning sectors, steam generators of nuclear plants or ORC cycles, and pipelines for petrochemical transportation.

Among two-phase flows, the annular two-phase flow is the most desired due to the intense heat transfer induced by the vapor core draining the thin liquid film at the wall. The knowledge of the relation between heat transfer and operating parameters is of primary importance for an accurate design in order to get the desired value of the heat transfer coefficient to balance the heat transfer resistances at each fluid side, being important to not exceed with the heat transfer intensity only at one side, since this would not be useful for the global thermal resistance, while penalizing considerably the pressure drops and the energy consumptions.

Several models have been developed to describe the behavior of an annular flow in literature, and it is well established that several concurrent factors affect the heat transfer and pressure gradients [6, 7]; they are related to the geometry (horizontal or vertical configuration, diameter and surface aspect),



thermophysical properties, liquid film thickness, liquid and vapor velocities, and liquid droplet entrainment.

The knowledge of the liquid film thickness at the wall is of primary importance to characterize an annular two-phase flow. In facts, simple models proposed in literature have successfully correlated the Nusselt number and the shear stress at the wall to the liquid film thickness [for example: 8, 9], which is directly related to the void fraction and the fraction of liquid entrained in the vapor core. Most of the models available in literature are based on the hypothesis of the symmetry (uniformity) of the liquid film distribution around the perimeter.

Applications of refrigerants to ORC cycles recovering waste heat and also a lot of plants working with fluids evaporating at a reduced saturation pressure close to 0.5 or higher are appearing. The operating conditions of these applications are outside the range of applicability of methods currently available. In facts, recent experimental studies have investigated this new range of operating conditions and have pointed-out the effect of gravity on heat transfer coefficients variation around the perimeter related to asymmetric liquid distribution at the wall [1, 2, 3] for horizontal flows.

Several works in literature deal with the determination of the liquid film thickness during annular flows.

Luninski *et al.* [10] measured the film thickness of air-water mixtures at different positions around the tube periphery, in channels with diameters ranging from 8.15 to 12.5 mm.

Ong and Thome [11] proposed a top/bottom liquid film thickness comparison for refrigerants R134a, R236fa and R245fa during flow boiling in small channels of 1.03, 2.20 and 3.04 mm diameter.

Other experiments were performed by Farias *et al.* [12], Fukano and Osaka [13], Laurinat and Hanratty [14], Masala *et al.* [15].

Cioncolini and Thome [16], Hurlburt and Newell [17] and Schubring and Shedd [18] proposed to predict quantitatively the evolution of eccentricity mainly for slightly stratified air-water flows.

In the studies of Cioncolini and Thome [16] and Schubring and Shedd [18], the eccentricity is defined as the ratio between top film thickness and bottom film thickness as shown by Eq. (1):

$$ecc_{ratio} = \frac{t_{top}}{t_{bottom}} \quad (1)$$

where t_{top} and t_{bottom} are respectively top and bottom film thicknesses.

Cioncolini and Thome [16] proposed a correlation for predicting the eccentricity ecc_{ratio} :

$$ecc_{ratio} = \frac{0.0789Fr_v^{1.90}}{1+0.0789Fr_v^{1.90}}; Fr_v > 1 \quad (2)$$

with

$$Fr_v = xFr_{vo}; Fr_{vo} = \frac{\frac{G}{\sqrt{\rho_{vap}}}}{\sqrt{g(\rho_{liq} - \rho_{vap})D}} \quad (3)$$

The correlation proposed by Schubring and Shedd [18] is defined as:

$$ecc_{ratio} = 1 - \exp(-0.63Fr_{ss}) \quad (4)$$

$$Fr_{ss} = \frac{xG}{\rho_{liq}(gt_{mean})^{0.5}} \quad (5)$$

with t_{mean} the mean film thickness calculated with the following empirical correlation:

$$\frac{t_{mean}}{D} = \frac{4.7}{x} \left(\frac{\rho_{vap}}{\rho_{liq}} \right)^{\frac{1}{3}} \left(\frac{GD}{\mu_{liq}} \right)^{-\frac{2}{3}} \quad (6)$$

Hurlburt and Newell [17] proposed a correlation to evaluate the grade of asymmetry at the bottom of the tube with respect to the mean film thickness on the circumference of the tube as follows:

$$ecc_{mean} = \frac{t_{mean}}{t_{bottom}} \quad (7)$$

The correlation proposed by Hurlburt and Newell [17] is:

$$ecc_{mean} = 0.2 + 0.7 \left(1 - e^{-\frac{1}{75} \left(\frac{x}{1-x} \right)^{0.5} Fr_{hn}^{-20}} \right) \quad (8)$$

valid for $\left(\frac{x}{1-x} \right)^{0.5} Fr_{hn} > 20$ and with $Fr_{hn} = \frac{xG}{\rho_{vap}(gD)^{0.5}}$

These predictive methods are based on data mostly related to air-to-water flows at ambient temperature, with large diameters (they range between 8.8 and 98 mm) and large excursions of the mass velocity; hence, they are calibrated in a large range of Froude numbers; on the other side these methods have been calibrated on a limited range of reduced pressures (mainly low reduced pressures) and they have not a good agreement with experiments at low mass fluxes or medium reduced pressures, as demonstrated in the assessment by Layssac *et al.* [5].

The work by Donniacuo *et al.* [3] showed experimental results during the evaporation of R245fa in a 2.95 mm horizontal tube. The operating conditions in which the experiments were performed are: mass velocities equal to 300 and 400 kg m⁻²s⁻¹ and saturation temperatures of 40, 60, 80 and 100°C. They experimentally showed that there is a combined effect of the Froude and Bond numbers on the stratification; the interrelationship being much evident at high reduced pressure or low mass fluxes. Recently, Layssac *et al.* [3] have proposed a correlation to account for the effects on the asymmetry both of the mass velocity, the diameter and of the thermodynamic properties.

The correlation proposed has the following form:

$$ecc_{diff} = \frac{2.7Fr_{vo}^{-1.2}\chi}{1+2.7Fr_{vo}^{-1.2}\chi} \text{ for } Fr_{vo}^{-1.2}\chi > 0.01 \quad (9)$$

$$ecc_{diff} \approx 0 \text{ for } Fr_{vo}^{-1.2}\chi \leq 0.01$$

where ecc_{diff} is defined as in the work by Donniacuo *et al.* [3] according to which the flow stratification is evaluated by considering the relative position of vapour core center compared to the flow center divided by internal radius as asymmetry parameter, whose strictly equivalent formula is:

$$ecc_{diff} = \frac{t_{bottom} - t_{top}}{D} \quad (10)$$

where D is the internal diameter, t_{bottom} and t_{top} respectively the bottom and the top film thicknesses. The limit cases of this definition correspond to a centered flow for an eccentricity of 0 and a full stratified flow with a bottom film thickness tending to the internal diameter when eccentricity is 1.

Equation (9) included the Martinelli parameter, related to the case of a turbulent-turbulent two-phase flow, defined as:

$$\chi = \left(\frac{1-x}{x} \right)^{0.9} \left(\frac{\rho_{vap}}{\rho_{liq}} \right)^{0.5} \left(\frac{\mu_{liq}}{\mu_{vap}} \right)^{0.1} \quad (11)$$

The Martinelli parameter is able to include the effect of the thermodynamic properties, which is important to have a predictive model able to capture predictions when there is a large variation of the reduced pressure. In fact, the paper [3] showed that this method is much more improved also when compared to a database of experiments including a large variation of the Froude number and of the thermodynamic properties (by means of the Martinelli parameter).

Layssac *et al.* [3] proposed a correlation, with no Bond number, Eq. (9), due to its weak influence in the statistics, since it ranged only from 11 to 18.

The aim of this work is to expand the range of operating conditions investigated previously to have a larger database, especially in those operating ranges that enlarge the effects of asymmetry and of the Bond number. In particular, the experiments were performed at mass flux velocities (G) from 50 to 300 kg m⁻²s⁻¹ and saturation temperatures (T_{sat}) of 20, 30, 40, 50° C, with Bond numbers from 8 to 10.

2. Experimental test facility, optical measurement technique and data reduction

The experimental test facility is well described in the work by Charnay *et al.* [1]. The same test bench was used to adjust the experimental conditions in terms of mass flow rate, vapor quality and saturation pressure at the inlet of the glass tube, placed at the end of the test section presented in Fig. 1(a).

The optical method used to measure the liquid film thickness is the same as that described in the paper presented by Donniacuo *et al.* [3]. A high-speed video camera system (Photron Fastcam SA3120KM2) enables the flow visualization by recording image sequences. The light system used for the visualization is provided through an adjustable light behind the visualization glass tube. The optical arrangement is a backlit imaging arrangement, resulting in a light gradient at the liquid–vapor interface due to shadowgraph effect. A high-speed camera system and a light behind the tube enable the visualization of the flow by recording frame sequences. The camera enables to get the local liquid film thickness with a mean resolution of 200 pixels.mm⁻¹.

In each condition of temperature and mass velocity, 4 series of 1363 frames are taken, corresponding to a total time of 2.7 s. The frame size is of 1024*1024 pixels and each pixel has a grayscale value ranging from 0 to 255. A MATLAB program has been conceived by Donniacuo *et al.* [3] which is able to get local film thickness for annular flows. An example of an image and the processing of the top and bottom thicknesses versus time is reported in Figure 1(b).

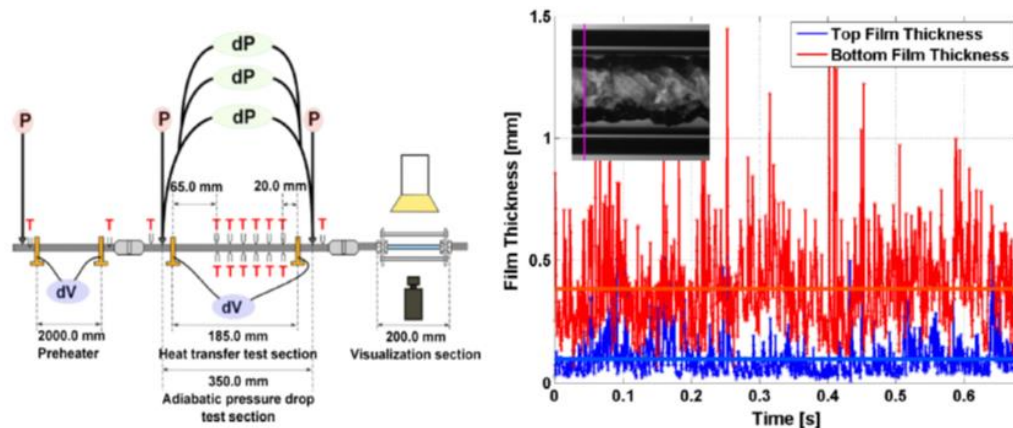


Figure 1. a) Schematic of the test facility. b) Local and average film thicknesses at saturation temperature of 80 °C, mass velocity of 300 kg m⁻² s⁻¹ and vapor quality of 0.35.

This method, based on grayscale analysis, has been improved to be applied to intermittent flows where single-phase profiles have to be detected by Layssac *et al.* [5], also permitting to sensibly reduce the uncertainty on interface detection for annular parts. Since the direct measurement suffers of the refraction effects through the glass of the tube, a correction factor was introduced. In case of intermittent flow the average value of the thickness is calculated only while there is a two-phase flow.

The uncertainty on the apparent film thickness is ± 2 pixels. At each operating condition, the top and bottom liquid film thicknesses were calculated as the average value from 5452 recorded frames. The uncertainty of each measurement is calculated, taking into account several sources of uncertainty: the inner and outer diameter dimensions, the variation of liquid R245fa refractive index with the temperature and the limitations of image resolution due to finite pixel dimensions. The combined uncertainty for film thickness measurement was evaluated as following:

$$\delta t_{real} = 2\sqrt{\left(\frac{\delta t_{app}}{EF.Sc}\right)^2 + \left(\frac{t_{app}\delta_{EF}}{-Sc.EF^2}\right)^2 + \left(\frac{t_{app}\delta_{Sc}}{-EF.Sc^2}\right)^2} \quad (12)$$

with t_{app} the apparent film thickness, t_{real} the real film thickness EF the enlargement factor due to optical deformation, and Sc the scaling factor. In the present study, $\delta t_{app} = 2$ pixels, $\delta_{EF} = 0.047$, $\delta_{Sc} = 0.84$ mm/pixel for an outer diameter of 909 pixels. As a conclusion, δt_{real} for the top film thickness ranges between 0.02 mm and 0.03 mm depending on the experimental conditions.

3. Experimental results

This paper presents experimental results during an adiabatic two-phase flow of the fluid R245fa in a smooth tube with an internal diameter of 2.95 mm, varying the mass flux, G , in the range 50-300 $\text{kg m}^{-2}\text{s}^{-1}$ and the saturation temperature from 20 and 50 $^{\circ}\text{C}$, in the whole range of vapour qualities.

Figure 2 (a)-(b) reports an example of the measured dimensionless top and bottom thicknesses as a function of the vapour quality at a constant mass flux, varying the Bond number from 8 to 10, where the Bond number is defined as:

$$Bd = \frac{g(\rho_{liq} - \rho_{vap})D^2}{\sigma} \quad (13)$$

including the effect of the variation of the saturation pressure, through the variation of the liquid and vapour densities with respect to the surface tension.

Consistently to the results of Donniacuo *et al.* [3] it is evident how the saturation pressure affects the dimensionless thickness, especially at the bottom of the tube and for low vapour qualities. In particular, increasing the saturation pressures the thickness at the bottom increasing for the same mass flux and vapour quality. This effect is present also at the top of the tube where the variation is less relevant.

In this work to evaluate the stratification a new parameter, S , the symmetry, is defined. S is the complement to 1 of the eccentricity, already defined by Eq. (10), as presented in the next equation

$$S = 1 - \frac{t_{bottom} - t_{top}}{D} \quad (14)$$

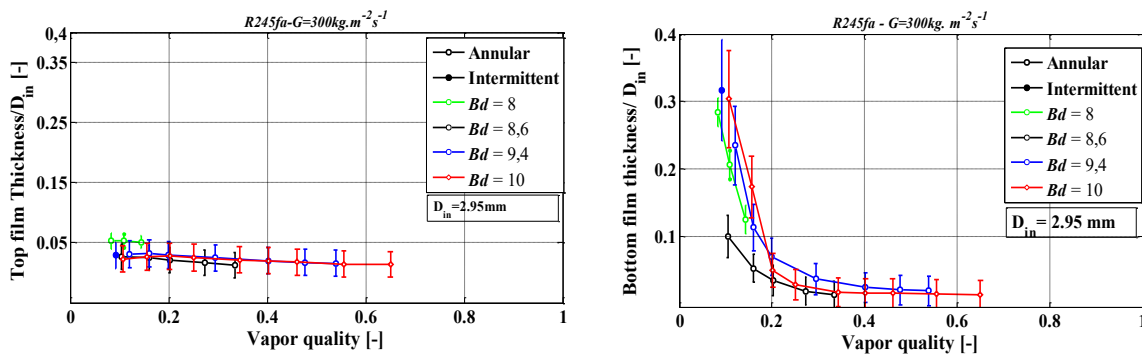


Figure 2. Dimensionless liquid film thickness at the wall for the fluid R245fa, an internal diameter of 2.95mm, a mass flux of $300 \text{ kg m}^{-2} \text{ s}^{-1}$, varying the Bond number from 8.0 to 10.0 (i.e. the saturation temperature from 20°C to 50°C). a) Measurements at the top of the tube. b) Measurements at the bottom of the tube.

When symmetry is equal to 1 there is no stratification, since the eccentricity is zero. On the contrary, zero is the expected value of the symmetry in case of higher stratification. This new parameter enables to organize the experimental results as shown in Fig. 3(a)-(b) which displays that symmetry tends to 1 when the vapour quality increases. The limit case of zero, geometrically corresponding to a bottom film thickness tending to the top side of the tube is not reached in the present case. First bubbles appearing with nucleation, the symmetry parameter was evaluated to 0.35. The symmetry parameter is thus more pertinent than the eccentricity as it enables to highlight the behaviour of centred and almost centred flows, while keeping the same mathematical limits.

During the experiments two different kinds of flow patterns were observed: annular flow and intermittent flow where the intermittent is considered as the combination of bubbly flow, bubbly-slug flow and slug flow.

At a fixed value of G , equal $200 \text{ kg m}^{-2} \text{ s}^{-1}$, by fixing also the value of the vapour quality, Fig. 3(a) shows the decline of symmetry when the Bond number is increasing from 8 to 10 and the vapour only Froude number is decreasing from 12 to 7.5. The definition of the vapour only Froude number used in this work is the one presented in Eq.(3)

The obtained trend of the symmetry, when these two dimensionless numbers are varying, is justified by the growth of T_{sat} .

Taking into account that the Bond number is the ratio between gravity and surface tension forces meanwhile the Fr_{vo} number is the ratio between inertia and gravity forces it is possible to resume that higher saturation temperature provides a higher Bond number and a lower Fr_{vo} number. This means higher stratification due to fact that the importance of the gravity forces is greater if compared to the surface tension and inertial forces.

Fig. 3(b) deals with the evolution of the symmetry at a Bond number equal to 8.6 with Fr_{vo} number varying from 2.6 to 15. A fixed value of Bond number implies that the saturation temperature is constant: the thermodynamic properties of the fluid do not change and consequently the buoyancy and surface tension forces are the same. Fr_{vo} number increases because of the growth of G and the only force rising is the inertial force. It is possible to see that when the Fr_{vo} number increases, symmetry increases that means lower stratification.

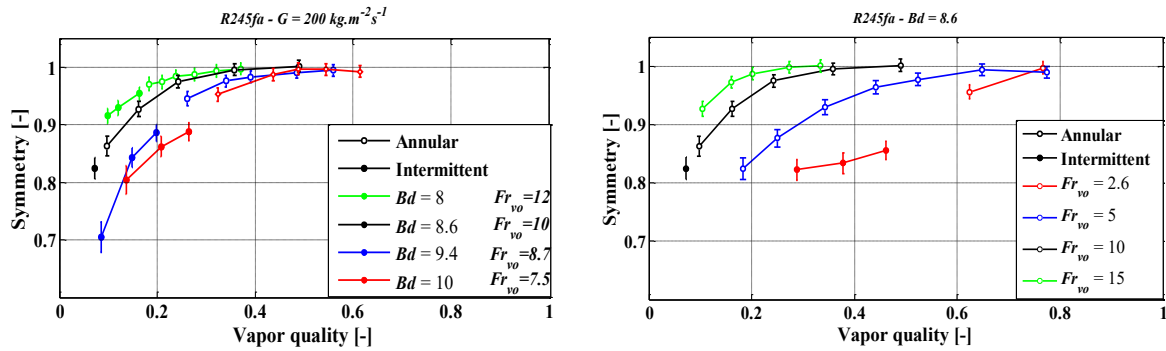


Figure 3. Plot of the experimental values of the symmetry parameter as defined in Eq. (14) as a function of the vapor quality, for the fluid R245fa. a) at $G=200 \text{ kg m}^{-2}\text{s}^{-1}$, varying the Bond number from 8.0 to 10; b) at Bond number equal to 8.6 and varying Fr_{vo} from 2.6 to 15.

The complement to 1 of the correlation proposed by Layssac *et al.* [5], introduced before in Eq.(9), provides a method for the prediction of the symmetry, as presented in the next equation. This method has an additional benefit to keep all the data points and to avoid an arbitrary limit for the value of $Fr_{vo}^{-1.2}\chi$ of 0.01 as presented in Layssac *et al.* [5]. The new correlation is:

$$S_{predicted} = 1 - ecc_{diff} = 1 - \frac{2.7Fr_{vo}^{-1.2}\chi}{1+2.7Fr_{vo}^{-1.2}\chi} \quad (15)$$

For a statistical analysis, the mean percentage error, MPE, and the mean average percentage error, MAPE, are considered. They are defined as follows:

$$MPE = \frac{1}{n} \sum_{i=1}^n \frac{S_{meas,i} - S_{pred,i}}{S_{meas,i}} \quad (16)$$

$$MAPE = \frac{1}{n} \sum_{i=1}^n \left| \frac{S_{meas,i} - S_{pred,i}}{S_{meas,i}} \right| \quad (17)$$

where n is the sample size, S_{meas} the experimental value of the symmetry and S_{pred} the predicted symmetry. MPE and MAPE obtained for the present data are respectively of -0.1% and 4.0%.

The comparisons of the measured values of the symmetry with the predictions of the new model, Eq. (14) are presented in Fig.4a) where it is possible to see that 94% of the available data points fall within $\pm 10\%$ error band.

Globally, it appears the present data points dispersion is slightly higher than in the case of Layssac *et al.* [5] experimental data while the mean predictions in both cases do not overestimate or underestimate the experimental data. The larger dispersion in present case can be related to the experimental conditions. Actually, the range of temperatures enables to reach a Bond number of 8, compared with the Layssac *et al.* [5] data which ranges from 11 to 18. This increases relative importance of surface tension effects on the two-phase flow, compared with buoyancy and inertia. Furthermore, the surface tension tends to replace inertia in mechanisms to centre the flow due to low mass velocity ($50 \text{ kg m}^{-2}\text{s}^{-1}$). Consequently, the new experimental data would not be well predicted for low mass velocity and low temperature since the geometry of the flow would be more conducted by surface tension compared with Layssac *et al.* [5] database.

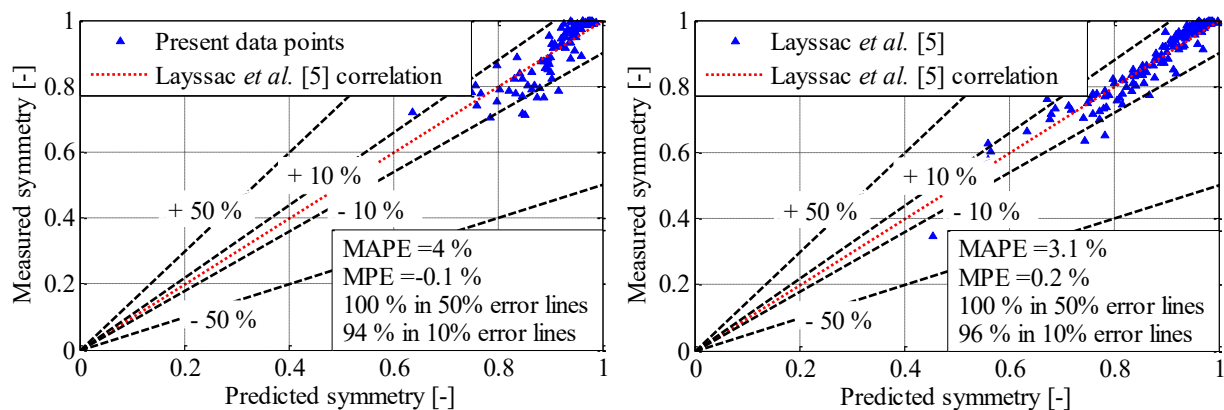


Figure 4. Plot of the statistical comparison between a) the new experimental results and the predictive method from equation (15); b) Layssac *et al.* [5] experimental results and the predictive method from equation (15).

4. Conclusions

New data points have been obtained on Charnay *et al.* [1] test facility. These points correspond to lower temperatures and lower mass velocities compared to the work led by Layssac *et al.* [5].

The general trend of two-phase flow symmetry was still well predicted by the analysis of dimensionless numbers such as vapour only Froude number and Bond number. Introduction of a new symmetry parameter enabled to easily analyze all types of flows, especially centred flows and then to avoid arbitrary limit for the field of application of the correlation of Layssac *et al.* [5].

The comparison between present experimental data and correlations has led to a larger dispersion with respect to the previous work by Layssac *et al.* [5], especially for not centred flows. This may be due to the higher relative importance of surface tension in the present conditions. Thus, it is planned to take into account these points, as well as bibliography data, in the optimization algorithm developed and described by Layssac *et al.* [5], in order to calibrate the correlation in a wider range of operating conditions. This would enable to highlight the contribution of surface tension in the correlation. Furthermore, the surface tension effect could be further analysed by reducing the internal diameter of the test section and by measuring the side film thicknesses.

References

- [1] Charnay R, Revellin R and Bonjour J 2015 Flow boiling heat transfer in minichannels at high saturation temperatures: Part I – Experimental investigation and analysis of the heat transfer mechanisms *International Journal of Heat and Mass Transfer* **87** 636-652
- [2] Mastrullo R, Mauro A W, Thome J R, Toto D and Vanoli G P 2012 Flow pattern maps for convective boiling of CO₂ and R410A in a horizontal smooth tube: Experiments and new correlations analyzing the effect of the reduced pressure *International Journal of Heat and Mass Transfer* **55** 1519-1528
- [3] Donniacuo A, Charnay R, Mastrullo R, Mauro A W and Revellin R 2015 Film thickness measurements for annular flow in minichannels: Description of the optical technique and experimental results *Experimental Thermal and Fluid Science* **69** 73-85
- [4] Mauro A W, Cioncolini A, Thome J R and Mastrullo R 2014 Asymmetric annular flow in horizontal circular macro-channels: Basic modeling of liquid film distribution and heat transfer around the tube perimeter in convective boiling *International Journal of Heat and Mass Transfer* **77** 897-905.
- [5] Layssac T Lips S and Revellin R 2016 Prediction of stratification during intermittent and annular flows of R245fa in an horizontal mini-channel *ICMF-2016 – 9th International Conference on Multiphase Flow* May 22nd –27th 2016 Firenze Italy.J.C.
- [6] Wallis G B 1969 *One-dimensional two-phase flow* McGraw-Hill New York.

- [7] Hewitt G F and Hall-Taylor N S 1970 *Annular two-phase flow* Pergamon Press, Oxford.
- [8] Asali J C, Hanratty T J and Andreussi P 1985 Interfacial drag and film height for vertical annular flow *AIChE Journal* **31** (6) 895-902.
- [9] Henstock W H and Hanratty T J 1976 The interfacial drag and the height of the wall layer in annular flows *AIChE Journal* **22** 990-1000.
- [10] Luninski Y, Barnea D and Taitel Y 1983 Film thickness in horizontal annular flow *Can. J. Chem. Eng.* **61** 621–626.
- [11] Ong C L and Thome J R 2011 Macro-to-microchannel transition in two-phase flow: Part 1 – Two-phase flow patterns and film thickness measurements *Experimental Thermal and Fluid Science* **35** 37–47.
- [12] Farias P S C , Martins F J W A , Sampaio L E B , Serfaty R and Azevedo L F A 2010 Liquid film characterization of horizontal, annular, two-phase, gas-liquid flow using time-resolved LASER-induced fluorescence *15th Int. Symp. on Applications of Laser Techniques to Fluid Mechanics* 5th-08th July Lisbon Portugal.
- [13] Fukano T and Ousaka A 1989 Prediction of the circumferential distribution of film thickness in horizontal and near-horizontal gas–liquid annular flows *Int. J. Multiphase Flow* **15** 403–419.
- [14] Laurinat J E, Hanratty T J and Jepson W P 1985 Film thickness distribution for gas-liquid annular flow in a horizontal pipe *PhysicoChem. Hydrodynam* **6** 179-195.
- [15] Masala T Harvel G and Chan J S Separated two-phase flow regime parameter measurement by a high speed ultrasonic pulse-echo system *Review of Scientific Instruments* **78**.
- [16] Cioncolini A and Thome J R 2013 Liquid film circumferential asymmetry prediction in horizontal annular two-phase flow *Int. J. Multiphase Flow* **51** 44-54.
- [17] Hurlburt E T and Newell T A 1997 Prediction of the circumferential film thickness distribution in horizontal annular gas-liquid flow *Air conditioning and refrigeration center Report ACRC TR-111* University of Illinois Urbana USA.
- [18] Schubring D and Shedd T A 2009 Critical friction factor modelling of horizontal annular base film thickness *Int. J. Multiphase Flow* **35** 389-397.

Nomenclature

Bd	Bond number	(-)	Abbreviations	
D	diameter	(m)	ORC	organic Rankine cycle
ecc	eccentricity	(-)	subscripts	
EF	enlargement factor	(-)	app	apparent
Fr	Froude number	(-)	bottom	bottom side
g	acceleration of gravity	(m s ⁻²)	diff	difference
G	mass flux velocity	(kg m ⁻² s ⁻¹)	EF	enlargement factor
MAPE	mean average percentage error	(%)	hn	Hurlburt and Newell method
MPE	mean percentage error	(%)	In	internal
S	symmetry	(-)	liq	liquid phase
Sc	scaling factor	(pixel mm ⁻¹)	mean	mean value
t	film thicknesses	(m)	pred	predicted value
T	temperature	(°C)	sat	saturation
x	vapor quality	(-)	Sc	scaling factor
greek letters			meas	measured value
μ	dynamic viscosity	(kg s ⁻¹ m ⁻¹)	ss	Schubring and Shedd method
ρ	density	(kg m ⁻³)	top	top side
σ	surface tension	(N m ⁻¹)	vo	as the cross section was filled only by the vapor
χ	Martinelli parameter	(-)	vap	vapour phase
			v	related to the vapor